Modeling the spatial variability of the shear strength of discontinuities of rock masses: application to a dam rock mass

D. Sow, C. Carvajal, P. Breul, L. Peyras, P. Rivard, C. Bacconnet, G Ballivy

MODELING THE SPATIAL VARIABILITY OF THE SHEAR STRENGTH OF DISCONTINUITIES OF ROCK MASSES: APPLICATION TO A DAM ROCK MASS

Djibril SOW [1], [2], [3]; Claudio CARVAJAL [2]; Pierre BREUL [3]; Laurent PEYRAS [2]; Patrice RIVARD [1]; Claude BACCONNET [3]; Gérard BALLIVY [1]

[1] Université de Sherbrooke, Sherbrooke, Québec, Canada,
{ Djibril.Sow2; Patrice.Rivard; Gerard.Ballivy } @USherbrooke.ca

[2] Irstea, UR RECOVER, Aix-en-Provence, France
{ laurent.peyras; claudio.carvajal } @irstea.fr

[3] Université Blaise Pascal, Clermont Ferrand, France
{ Pierre.Breul; Claude.Bacconnet } @polytech.univ-bpclermont.fr

ABSTRACT

The shear strength of discontinuities plays a key role in the stability of rock masses, particularly in the case of analyzing the sliding stability of the rock foundations of gravity dams. This paper proposes a methodology for analyzing the spatial variability of shear strength along the joints of rock mass, based on the input parameters of the Barton and Choubey's model. The aim of this approach is to evaluate the reduction of the variance of the parameters involved at full-scale by identifying a deterministic trend varying in depth and a spatial correlation calculated from a variographic analysis. An advantage of this methodology is to use a simple experimental protocol (a laser profilometer, a portable shear test apparatus and a concrete sclerometer), which generates large sets of shear strength properties for assessing their spatial variability. The methodology is illustrated in the case of the rock foundation of a concrete gravity dam. Analysis of the spatial variability conducted for this case study led to a significant reduction of the variance of the variable analyzed. The advantage of this method is demonstrated through the evaluation of the probability of failure performed in a study of this structure's stability. Taking variance reduction into account in the case study led to significantly reducing the probability of failure assessed through a reliability analysis.

Keywords: rock joints, gravity-dam, rock foundation, shear strength, spatial variability, geostatistic.

1   INTRODUCTION

The shear strength of discontinuities plays a key role in the stability of rock masses, particularly in the case of analyzing the sliding stability of the rock foundations of gravity dams. Rock masses often present vertical and horizontal variability regarding the shear strength properties of their joints (Phoon and Kulhawy 1999). The question of characterizing the spatial variability of the shear strength of rock masses appears crucial for providing a more satisfactory evaluation of their stability, since doing so would lead to reducing the variance of strength properties in limit state calculations and thus to optimizing the stability assessment. Indeed, taking into account the reduction in the variance of strength properties permits optimizing the estimation of: i) the values of conservative calculations for deterministic justifications, ii) the characteristic values corresponding to a fractile in semi-probabilistic justifications (Peyras et al., 2010), iii) the variance of random strength variables in probabilistic justification (Vanmarcke, 1983; Carvajal et al. 2009).

The variance of shear strength properties involved at the joint scale is lower than that evaluated at the laboratory scale. This reduction of variance results from the larger surface involved (linked to an average of punctual values) and from the spatial correlation of shear strength properties. Analyzing spatial variability through random fields makes it possible to take this reduced variance into account (Gravanis et al., 2014, Vanmarcke, 1983).

Several authors have focused on modeling the spatial variability of rock masses, such as (Duzgun et al., 2002), (Gravanis et al., 2014) and (Shamekhi et al., 2015). (Duzgun et al., 2002) proposed a probabilistic model to estimate the in-situ shear strength of rock joints based on shear strength measurements obtained in the laboratory. (Gravanis et al., 2014) put forward an analytical solution for the probabilistic evaluation of rock mass slope stability. The methodology proposed by (Gravanis et al., 2014) was based on random fields defined for the shear strength parameters of the Mohr-Coulomb criterion and was applied to the case of a joint along a predefined flat surface. (Shamekhi et al., 2015) also proposed a probabilistic method for evaluating the slope stability of a rock mass, in which the variability of the geometric properties of the joints were taken into account in a finite element model.

Modeling the spatial variability of a soil/rock strength property can be a difficult task because the number of test data obtained during site investigation is usually too sparse to carryout meaningful statistical analysis. Bayesian methods have been recently developed to address this issue in geotechnical and rock engineering (e.g., Wang and Cao 2013, Wang and Aladejare 2015, Wang et al. 2016).

Performing direct shear tests provides reference data for quantifying the shear strength of joints. However, these tests are expensive and only a limited number are performed with the test pieces available, which does not provide a statistically representative range of samples of the dispersion of shear strength properties. To solve this, we proposed a modified procedure using the Barton and Choubey's criterion (1977) to characterize joint shear strength (Sow et al., 2015). Our methodology is based on an experimental approach that uses simple resources to determine the parameters of the Barton and Choubey criterion: a laser profilometer, a portable shear test device and a concrete sclerometer. This experimental approach generates large sets of shear strength properties, through the application of a simple and inexpensive experimental protocol. The statistical sample of shear strength properties thus generated can then be analyzed and the spatial variability modeled.

The present paper continues in this direction in view to developing a methodology for analyzing the spatial variability of the shear strength of the joints of rock masses. The proposed methodology, based on the input parameters of the Barton and Choubey's model

1 aims to evaluate the effects of reduced variance of the shear parameters involved in limit state
2 calculations (Sow, 2015). An advantage of this methodology is to use a simple experimental
3 protocol (a laser profilometer, a portable shear test apparatus and a concrete sclerometer),
4 which generates large sets of shear strength properties for assessing their spatial variability.

5 The methodology proposed to analyze spatial variability comprises the following steps:

6 – The probabilistic description of the joints of a rock mass on the basis of a stereographic
7 analysis;
8 – Using the Barton and Choubey criterion to characterize joint shear strength;
9 – Modeling spatial variability at the scale of the sample (from core samples) of
10 parameters measured in the experimental campaign and the parameters of the Barton
11 and Choubey criterion. Modeling the variability of the parameters studied highlights a
12 deterministic trend as a function of spatial localization, a random measurement error
13 variable and random error variable of the model linked to a deterministic trend;
14 – Modeling the spatial variability at the scale of the structure of the rock joint shear
15 strength parameters on the basis of a variance reduction analysis.

16 The first two steps have already been used or published in the scientific literature to
17 analyze rock masses and joint shear strength and are developed briefly in the first part of this
18 paper. The second part of the paper presents the core of the methodological developments
19 proposed to model the spatial variability of the joint shearing parameters. The methodology is
20 illustrated in the third part of this article using the example of a rock foundation of a concrete
21 gravity dam situated in Canada. Its efficiency is demonstrated through the presentation of a
22 reliability analysis of the shear strength of a dam rock mass with a geo-modeling application
23 using the finite elements method. The article ends with a discussion on the methodology and
24 the results.

25 ## 2 MATERIAL AND METHODS

26 This section briefly describes the tools and the methods already available in the literature
27 that will be used in the methodology proposed in this paper in order to model the spatial
28 variability of the shear strength of the discontinuities.

29 ### 2.1 Probabilistic description of the joints of a rock mass

30 Rock masses are usually jointed heterogeneous media encompassing two types of
31 element: rock blocks and joints. Due to their low stiffness, low strength regarding certain
32 stresses (shear) and their hydraulic conductivity, joints play a predominant role in the
33 behavior of rock masses (Panet, 1976).

34 The parameters that allow describing joint geometries are orientation, spacing and
35 persistence (Blès, 1981).

36 The joints of a rock mass do not have a random orientation and are often organized in
37 directional sets whose number is linked to the geological and mechanical phenomena
38 involved during its formation and tectonic history (AFTES, 2003).

39 A stereographic projection was used for studying the distribution of joints in directional
40 sets. When the different sets have been identified, we then analyze each set statistically by
41 creating histograms of the distribution of geometric parameters relating to orientation, spacing
42 and persistence (Hoek and Brown 1980, AFTES 2003).

1   This probabilistic description of the joints of a rock mass provides the input data for the
2   geomodelers and permits simulating the spatial distribution of the joints.

3   ## 2.2 Available data and the joint shear strength criterion

4   The shear strength developed along the joints can be evaluated using two different
5   approaches. The first entails direct shear testing while the second the use of an empirical
6   failure criterion corresponding to a shear strength envelope (ISRM, 1978).

7   The shear strength evaluated by direct shear tests on rock joints is a reference
8   experimental approach (Panet 1976, ASTM D5607-08 2008). However, the experimental
9   procedures associated with these tests lead to obtain a limited number of samples available
10 and therefore characterizing the shear strength variability of the rock studied.

11 The second approach uses empirical failure criteria and employs experimental protocols
12 that are often quick and simple to use. The use of empirical failure criteria makes it possible
13 to acquire shear data and get round the problem linked to the representativeness of the
14 sampling (Grasselli and Egger, 2003). These empirical failure criteria include the Barton and
15 Choubey's model (1977), which is recommended by the ISRM (1978) and remains widely
16 used in engineering (Tatone and Grasselli 2012).

17 In our approach, the Barton and Choubey's criterion was used to characterize the joint
18 shear strength. This criterion (equation [2]) introduces a parameter that takes roughness into
19 account called *JRC* (*Joint Roughness Coefficient*), a mechanical strength parameter, *JCS*, that
20 takes rock alteration into account (*Joint Compressive Strength*) and the residual friction angle,
21 denoted φ_r. The term σ_n represents the normal stress and τ_{pic} the peak shear strength.

22
$$\tau_{pic} = \sigma_n \tan\left(\varphi_r + JRC \log_{10}\left(\frac{JCS}{\sigma_n}\right)\right)$$
[1]

23 The experimental protocols for evaluating Barton and Choubey (1977) parameters can be
24 performed easily on almost every joint or test piece obtained from coring. The methodology
25 chosen for our research is based on an experimental approach (Sow *et al.*, 2015) which uses
26 fewer resources in comparison to classical shear tests to determine the parameters of the
27 Barton and Choubey criterion: a concrete sclerometer to evaluate the *JCS* parameter, a
28 portable shear test device to determine φ_r and a laser profilometer to scan the surface to
29 evaluate the *JRC*.

30 The parameters measured directly by this experimental methodology are: i) the rebound
31 values of altered and non-altered joints, *r* and *R* obtained using the Schmidt hammer; ii) the
32 basic friction angle φ_b obtained by shear testing of sawn joints; iii) the statistical roughness
33 parameter Z_2 (likened to the average slope of the scanned profile).

34 At the end of the experimental campaign, the Barton and Choubey (1977) input
35 parameters are evaluated using the following empirical models:

36
$$\varphi_r = (\varphi_b - 20) + 20 * \frac{r}{R}$$
[2]

37
$$JCS = 9.97 * e^{(0.02*R*\rho)}; \text{ with } \rho: \text{rock matrix density}$$
[3]

38
$$JRC = 32,2 + 32,47.\log(Z_2)$$
[4]

4

1   These empirical models [2, 3, 4] were proposed by Barton & Choubey (1977) for φ_r,
2   Deere & Miller (1966) for *JCS* and Tse & Cruden (1979) for *JRC*.

3   This methodology was subjected to a comparison with the results of measures performed
4   with 35 direct shear tests (Sow *et al.*, 2015), on altered and non-altered joints, tested under
5   normal stresses varying from 0.15 to 2 MPa (stresses generally found in dam foundations). In
6   this comparison, the approach suggested by (Sow *et al.*, 2015) led to a good estimation of the
7   shear strength, with a small deviation (about 7%) in comparison with direct shearing tests. It
8   has the advantage of using relatively simple experimental protocols, making it possible to
9   obtain sufficiently abundant data to then carry out a statistical analysis of spatial variability.

10 ## 2.3 Modeling spatial variability using geostatistical methods

11   The purpose of a geostatistical approach is to model a random variable varying
12 continuously in a fixed spatial domain (Matheron, 1970). With this approach, the
13 characterization and modelling of the spatial variations of the variable studied are performed
14 with variograms.

15   We consider a random variable $Z(.)$, a spatial domain D, and a sample of measures $Z(s_1)$,
16 $Z(s_2)$, …, $Z(s_n)$, where s_1, s_2, …, s_n represent the spatial position or the site where the measures
17 are performed. The variogram is a tool that characterizes the spatial dependence of the
18 variable $Z(.)$ in domain D. The theoretical variogram $\gamma(h)$ is defined as:

19
$$\gamma(h) = 0.5\,Var[Z(s) - Z(s + h)] = 0.5\,E[(Z(s) - Z(s + h))^2] \qquad [5]$$

20   where *Var* and *E* represent the variance and the expected value respectively, *s*
21 corresponds to the coordinates and *h* is the distance between the points.

22   The *nugget effect* is defined as the value taken by the variogram $\gamma(h)$ when *h* draws close
23 to the origin. When *h* increases, the variogram may or may not reach a plateau. Reaching a
24 plateau indicates that counting from a certain distance, spatial dependence no longer exists
25 between the data. This distance is called *range* and the term *sill* denotes the variance at which
26 the plateau appears. This sill corresponds to the variance of variable $Z(.)$, also denoted σ_Z^2.
27 The relation between the covariance function $C(h)$ and the variogram $\gamma(h)$ when it reaches a
28 sill is the following:

29
$$C(h) = \sigma_Z^2 - \gamma(h) \qquad [6]$$

30   The variogram can be built experimentally from a sample of spatially localized measures.
31 Finally, the experimental variogram can be fitted to the theoretical model.

32

3   THEORY AND CALCULATION

This section presents the methodology proposed to model the spatial variability of shear strength parameters of rock joints. The approach used here to analyze the spatial variability of joint shear strength includes the following parameter modeling steps:

1. Modeling the variability of the parameters measured at the scale of the joints intersected by vertical boring;
2. Modeling the variability of the input parameters of the Barton and Choubey model, determined using an empirical model, at the scale of the joints intersected by boring;
3. Modeling the variability of the input parameters of the Barton and Choubey model integrated at the scale of the limit state (scale of the structure).

3.1   Modeling the variability of the measured parameters

3.1.1   Definition and discretization of regionalized variables $Z_i(x)$

We denote $Z_i(x)$ the regionalized variables corresponding to the parameters measured at the scale of the joints intersected by boring, where x corresponds to the coordinate or vertical position in the borehole. It includes:

- the rebound value of the rock matrix $R(x)$ and the altered joints $r(x)$ obtained using a Schmidt hammer;
- the basic friction angle $\varphi_b(x)$ obtained by the shear test on the sawn joints;
- the statistical roughness parameter $Z_2(x)$ evaluated on the surfaces of the joints scanned with a laser profilometry.

In our approach to parameter variability modeling, we propose discretizing and formulating the regionalized variables $Z_i(x)$ as the sum of independent variables:

- a deterministic trend as a function of spatial localization $t_{Zi}(x)$;
- a variable of fluctuation around the non-biased trend $w_{Z_i}(x)$;
- a random non-biased measurement error variable e_{Z_i} (Vanmarcke 1983, Phoon *et al.*, 1999).

$$Z_i(x) = t_{Z_i}(x) + w_{Z_i}(x) + e_{Z_i} \qquad [7]$$

3.1.2   Modeling of the deterministic trend as a function of spatial localization $t_{Zi}(x)$

We determine the trend $t_{Zi}(x)$ of a parameter (the rock matrix rebound value R and altered joints r, the basic friction angle φ_b and the statistical roughness parameter Z_2) with a linear regression on the quantitative data of $Z_i(x)$ according to the depth of the borehole and taking into account the qualitative data of observations of borehole logs. The aim is to consider that the variability of the properties of a rock mass is not totally random and that part of this variability can be explained by physical phenomena and represented by a deterministic trend.

1   ### 3.1.3   Modeling the random measurement error variable e_{Zi}

2   We model the measurement errors e_{Z_i} as zero mean random variables and of non-zero
3   variance (Phoon *et al.*, 1999, Favre 2004). Quantifying the variance of the measurement error
4   is closely linked to the experimental protocol associated with the parameter measurement. We
5   characterize the measurement error intrinsic to the test by the variance of the results obtained
6   from a representative number of runs of this experimental protocol on nominally identical
7   samples.

8   The measurement of the rebound value R and r corresponds to the mean of 10 higher
9   values $\{R_{10}\}$ or $\{r_{10}\}$ obtained from 20 Schmidt hammer impacts on the surface of a sample.
10   The measurement error is associated with the uncertainty on the estimation of the mean of
11   these 10 higher values. Thus we propose estimating the variance of the measurement error of
12   R and r by the sampling error according to equation [8]:

13
$$\text{Var}[e_R] = \frac{\text{Var}[\{R_{10}\}]}{10} \qquad [8]$$

14   To determine the basic friction angle φ_b, the technical recommendations state that shear
15   tests should be carried out on a smooth joint with 8 steps of increasing normal stress (Gyenge
16   et Herget 1977). We estimate the variance of the measurement error φ_b by the variance of the
17   angles associated with each of these steps.

18   The measurement error on parameter Z_2 obtained from the laser scans was omitted given
19   the high precision provided by this device.

20   ### 3.1.4   Modeling the trend fluctuation variable $w_{Zi}(x)$

21   We consider the random fluctuation $w_{Z_i}(x)$ as a zero mean variable and of non-zero
22   variance (Phoon *et al.*, 1999, Favre 2004). Its characterization consists in evaluating its
23   variance and spatial correlation. We determine the variance of $w_{Z_i}(x)$ from the variance of
24   fluctuation $\left[Z_i(x) - t_{Z_i}(x)\right]$ and the variance of the measurement error e_{Z_i} :

25
$$\text{Var}\left[w_{Z_i}(x)\right] = \text{Var}\left[Z_i(x) - t_{Z_i}(x)\right] - \text{Var}\left[e_{Z_i}\right] \qquad [9]$$

26   We characterize the spatial correlation of $w_{Z_i}(x)$ with the variance reduction coefficient
27   $\Gamma_{Z_i}^2(L_v)$. It is likely determined from the experimental variogram of the values of $w_{Z_i}(x)$.
28   However, it is impossible to determine on each measured value of $Z_i(x)$, the share proper to
29   the test error e_{Z_i}. It is nonetheless noteworthy that the measurement error is by definition,
30   proper to the test and so it should not present a spatial correlation. Therefore we suggest
31   calculating the variogram directly from the data $\left[w_{Z_i}(x) + e_{Z_i}\right]$.

32   ## 3.2   Modeling the variability of input parameters of the Barton and
33   Choubey model at the scale of the joints intersected by a borehole

34   We denote $Z_{di}(x)$ the input parameters of the Barton and Choubey model at the scale of
35   the joints intersected by the borehole, corresponding to parameters $\{JRC(x), JCS(x)$ and
36   $\varphi_r(x)\}$. They are determined using an empirical model T_i and measured parameters $Z_i(x)$.
37   This empirical model T_i introduces an error assumed to be free of bias ε_i on parameter
38   $Z_{di}(x)$. However, this model error is difficult to characterize. It can be assessed by a
39   regression analysis of the models proposed in the literature; however, detailed input data of

1   these models is rarely available. The model error can also be assessed by comparing the
2   values estimated by a model and the values obtained experimentally (which are rarely
3   available in large numbers). Taking into account the model errors requires special
4   developments, which constitute a goal to improving the methodology proposed in this article.

5
$$Z_{di}(x) = \ T_i(Z_1(x); \dots.; Z_n(x); \ \varepsilon_i) \tag{10}$$

6   The empirical models used in our study to evaluate the input parameters of the Barton
7   and Choubey criterion from the values measured in our experimental campaign are presented
8   by equations [2] to [4].

9   Monte Carlo simulations or a Taylor series can be used to estimate the expected value
10 and the variance of the input parameters of the Barton and Choubey model at the joint scale
11 $Z_{di}(x)$. The latter is an approximation whose advantage is that it allows an analytical
12 calculation of the expected value and the variance of variables $Z_{di}(x)$, which is more practical
13 in engineering.

14 The following equations [11] to [13] present the analytical formulas for estimating the
15 expected value E[...] of the input parameters of the Barton and Choubey criterion at the scale
16 of the joints obtained from Taylor series linearization:

17
$$E[JRC(x)] = 32.2 + 32.47\log\left(t_{Z_2}(x)\right) \tag{11}$$

18
$$E[JCS(x)] = 9.97 * e^{(0.02*t_r(x)*\rho)} \tag{12}$$

19
$$E[\varphi_r(x)] = \left(t_{\varphi_b}(x) - 20\right) + 20 * \frac{t_r(x)}{t_R(x)} \tag{13}$$

20 The equations [14] to [19] present the analytical formulas for estimating the variances
21 *Var*[…] of the input parameters of the Barton and Choubey criterion at the scale of the joints
22 obtained from Taylor series linearization:

23
$$Var[JRC(x)] = \left(\frac{32.47}{\ln(10)*t_{Z_2}(x)}\right)^2 Var\left[w_{Z_2}(x)\right] \tag{14}$$

24
$$Var[JCS(x)] = \left(0.2 * \rho * e^{[0.02*\rho*t_r(x)]}\right)^2 (Var[w_r(x)] + Var[e_r]) \tag{15}$$

25
$$Var[\varphi_r(x)] = Var\left[w_{\varphi_r}(x)\right] + Var\left[e_{\varphi_r}\right] \tag{16}$$

26 with:

27 $$Var\left[w_{\varphi_r}(x)\right] = Var\left[w_{\varphi_b}(x)\right] + a_1(x)^2 \cdot Var[w_R] + a_2(x)^2 \cdot Var[w_r(x)] - a_3(x) \cdot$$
28 $$Cov\left(w_R(x); w_r(x)\right) \tag{17}$$

29
$$Var\left[e_{\varphi_r}\right] = Var\left[e_{\varphi_b}\right] + [a_1(x)^2 + a_2(x)^2 - a_3(x)] \cdot Var[e_R] \tag{18}$$

30 Where:

31
$$a_1(x) = \frac{20*t_r(x)}{t_R(x)^2}; \ \ a_2(x) = \frac{20}{t_R(x)}; \ \ a_3(x) = \frac{800*t_r(x)}{t_R(x)^3} \tag{19}$$

32

3.3 Modeling the variability of the input parameters of the Barton and Choubey model at the scale of the limit state

The geotechnical parameter to consider in the analysis of a limit state is that which is integrated on the entire area mobilized by the failure mechanism (Favre 2004). We denote $Z_L(L)$ the input parameters of Barton and Choubey's model integrated at the scale of the limit state (scale of the structure) along the portion of the borehole (portion with length L) affected by the limit state: $\{JRC_L(L); JCS_L(L); \varphi_{r_L}(L)\}$, with:

$$Z_L(L) = \frac{1}{L}\int_0^L Z_{di}(x)\,.\,dx \qquad [20]$$

The following equations [21] à [23] present the analytical formulas for estimating the expected value $E[\ldots]$ of the input parameters of the Barton and Choubey criterion at the scale of the structure, obtained by Taylor series linearization:

$$E[JRC_L(L)] = 32.2 + 32.47\frac{1}{L}\int_0^L \log\left(t_{Z_2}(x)\right)\cdot dx \qquad [21]$$

$$E[JCS_L(L)] = \frac{1}{L}\int_0^L 9.97 * e^{(0.02*\rho*t_r(x))}\cdot dx \qquad [22]$$

$$E\left[\varphi_{r_L}(L)\right] = \frac{1}{L}\int_0^L \left[\left(t_{\varphi_b}(x) - 20\right) + 20*\frac{t_r(x)}{t_R(x)}\right]\cdot dx \qquad [23]$$

We propose a geostatistical analysis to determine the variance reduction coefficient from the variograms obtained with regionalized variables, so the variance of the different input parameters of the Barton and Choubey's model can be determined at the scale of the limit state.

Equation [24] allows estimating the variance of variable $JCS_L(L)$:

$$\mathrm{Var}[JCS_L(L)] = \left(\frac{1}{L}\int_0^L 0.2*\rho*e^{[0.02*\rho*t_r(x)]}\cdot dx\right)^2 * \left(\Gamma_r^2(L)*\mathrm{Var}[w_r(x)] + \mathrm{Var}[e_r]\right) \quad [24]$$

- with $\Gamma_r^2(L)$ being the variance reduction coefficient of the fluctuation variable $w_r(x)$ obtained from the variogram calculation.

The variance of variable $JRC_L(L)$ is estimated with equation [25] :

$$\mathrm{Var}[JRC_L(L)] = \Gamma_{Z_2}^2(L)*\mathrm{Var}\left[w_{Z_2}(x)\right] * \left[\frac{1}{L}\int_0^L\left(\frac{32.47}{\ln(10)*t_{Z_2}(x)}\right)\cdot dx\right]^2 \qquad [25]$$

- with $\Gamma_{Z_2}^2$ being the variance reduction coefficient of the fluctuation variable w_{Z_2} obtained from the variogram calculation.

Equation [26] permits estimating the variance of variable $\varphi_{r_L}(L)$:

$$\mathrm{Var}\left[\varphi_{r_L}(L)\right] = \mathrm{Var}\left[w_{\varphi_{rL}}(L)\right] + \mathrm{Var}\left[e_{\varphi_{rL}}(L)\right] \qquad [26]$$

- with:

$$\text{Var}\big[w_{\varphi_{rL}}(L)\big] = \Gamma_{\varphi_b}^2(L) * \text{Var}\big[w_{\varphi_b}(x)\big] + \Gamma_R^2(L) * \text{Var}[w_R(x)] \cdot \left[\frac{1}{L}\int_0^L a_1(x) \cdot dx\right]^2 + \Gamma_r^2(L)$$

$$* \text{Var}[w_r(x)] \cdot \left[\frac{1}{L}\int_0^L a_2(x) \cdot dx\right]^2$$

$$- \text{Cov}\big(\Gamma_R^2(L) \cdot w_R(x); \Gamma_r^2(L) \cdot w_r(x)\big)\frac{1}{L}\int_0^L a_3(x) \cdot dx$$

1 [27]

$$\text{Var}\big[e_{\varphi_{rL}}\big] = \text{Var}\big[e_{\varphi_b}\big] + \text{Var}[e_R] \cdot \left[\frac{1}{L}\int_0^L a_1(x) \cdot dx\right]^2 + \Gamma_r^2 + \text{Var}[e_R] \cdot \left[\frac{1}{L}\int_0^L a_2(x) \cdot dx\right]^2$$

$$- \text{Var}[e_R]\frac{1}{L}\int_0^L a_3(x) \cdot dx$$

2 [28]

3   It is noteworthy that the variograms allow obtaining variance reduction coefficients built
4 for fluctuation values around the deterministic trend $Z_i(x) - t_{Z_i}(x)$. We consider this
5 fluctuation variable to be free of bias and stationary, thereby permitting the use of variograms.

6 **4   CASE STUDY AND RESULTS**

7 **4.1   The rock mass studied and spatial data**

8   The case study analyzed is the rock mass of an existing gravity dam with a maximum
9 height of 30 m above the natural terrain. The direction of the dam axis is 110°, i.e. close to an
10 east-west strike.

11   The rock mass is biotite granite gneiss of subdomain M4 of the Mékinac group. Unit M4
12 is composed of gneiss and composite gneiss. The rock mass exhibits three sets of joints: a set
13 of joints developed along the foliation (set 1) and two sub-vertical sets (set 2 and 3). The
14 statistical analyses of these joints led to modeling the distribution of the orientation and
15 spacing parameters using a Langevin-Fisher law and an exponential law, respectively. The
16 results of this analysis are summarized in Table 1.

17

	Orientation parameters			Spacing	
Joint set	Mean dip (°)	Mean direction of dip (°)	Parameter K (Langevin-Fisher law)	Mean spacing (m)	Parameter λ (exponential law)
Set 1	16	99	42	0.22	4.55
Set 2	85	172	40	0.84	1.20
Set 3	85	238	55	1.37	0.73

18   **Table 1 : Results of the statistical analysis of orientation and spacing parameters**

19

1   Four vertical boreholes of about 8 meters deep in the rock mass were drilled. Samples of
2 rocks and joints were recovered from these boreholes, referenced by depth. The following
3 tests were conducted:

4   – 62 Schmidt hammer tests: 52 and 10 tests to determine the rebound value R and r
5   respectively;

6   – 19 shear tests on smooth joints (φ_b);

7   – 19 surface scans with a laser profilometer (Z_2).

8

9 4.2   Results relating to the spatial variability of shear strength parameters

10   Here, we implement the proposed methodology to the case study in order to analyze the
11 spatial variability of the shear strength properties of rock joints.

12 4.2.1 Modeling the parameters measured

13   Table 2 summarizes the statistical analysis of the parameters measured experimentally
14 (without spatial variability into account):

15

Parameter	r [-]	R [-]	ϕ_b [°]	$Z2$ [-]
Mean	42.97	50.29	32.47	0.184
Standard deviation	5.39	3.89	1.98	0.036
Variation coefficient	0.13	0.08	0.06	0.197
Variance	29.03	15.14	3.93	0.001

16   **Table 2 : Statistical data of the measured parameters**

17

18   The measurements of r are on average lower than R given the alteration, but they present
19 greater dispersion.

20   Figure 1 shows the results of the parameters measured as a function of depth x under the
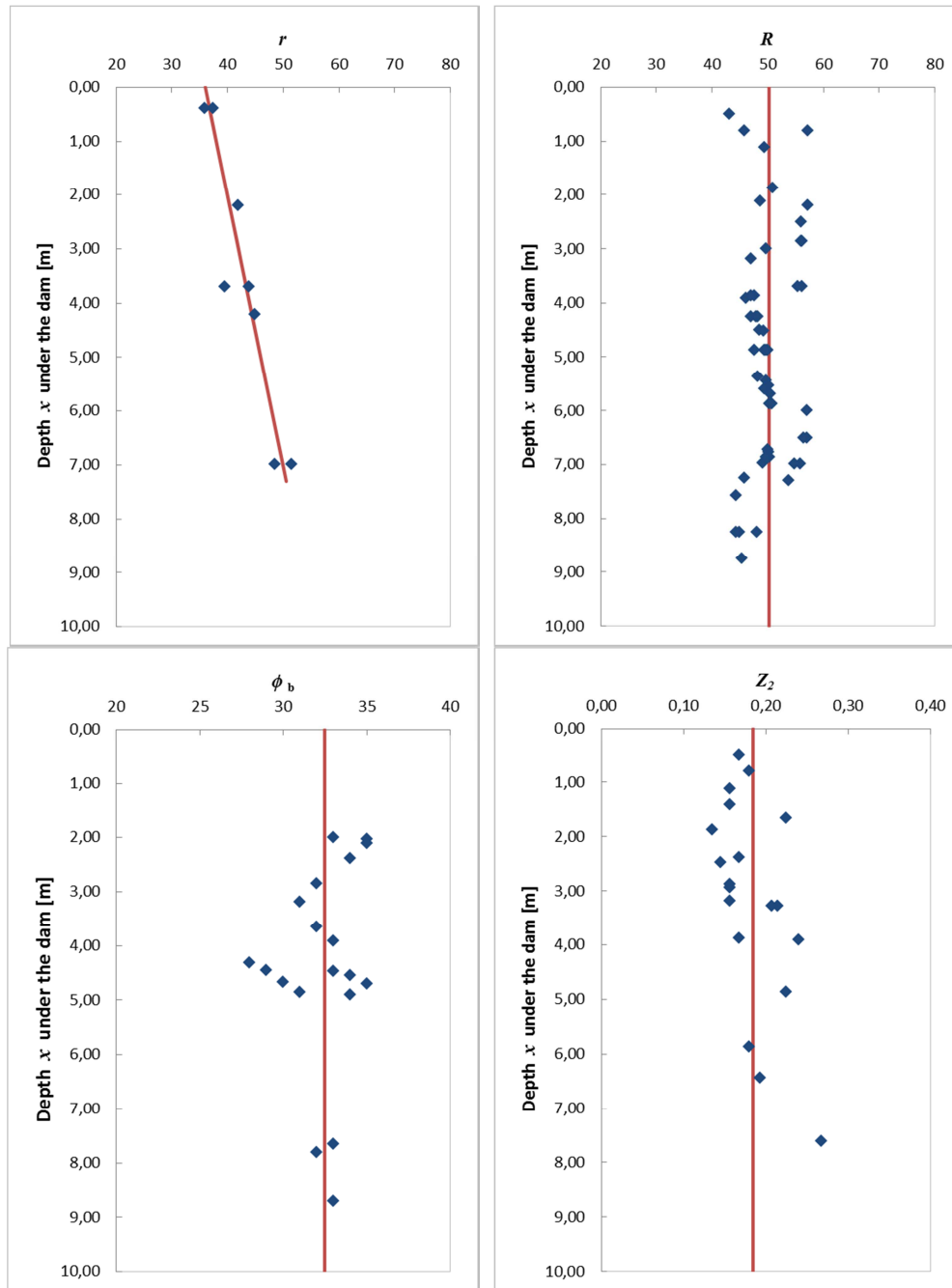21 dam-rock interface and the representation of a trend $t_Z(x)$ estimated by linear regression.

22

1

2

3   **Figure 1: Parameters measured as a function of the depth under the dam-rock interface.**

4

5   The data available for the rebound values of the altered joints $r(x)$ were less plentiful than
6   the rebound values of the rock matrix $R(x)$. However, they allowed observing an increasing
7   trend as a function of depth for the rebound values of the altered joints $r(x)$. This increase was
8   observed down to a depth of about 6 m (limit of the data available on r) where the rebound
9   value of the altered joints was close to the mean value observed for the joints of the rock
10   matrix R.

11   For the other parameters (basic friction angle φ_b and the statistical roughness value Z_2),
12   we did not identify the net trend thus it was therefore reasonable to adopt a constant value
13   equal to the mean for the deterministic trend $t_z(x)$.

1 For each of the parameters measured Table 3 presents the variances of variables
2 representing:

3 - the fluctuation or total deviation between the measured values and the deterministic
4 trend $[Z_i(x) - t_{Z_i}(x)]$;
5 - the measurement error e_{Z_i};
6 - the difference between the latter, $w_{Z_i}(x)$.

7

Parameter Z_i	r [-]	R [-]	ϕ_b [°]	$Z2$ [-]
$Var[Z_i(x) - t_{Z_i}(x)]$	3.41	15.14	3.93	0.001
$Var[e_{Z_i}]$	0.59	0.59	0.005	~0
$Var[w_{Z_i}(x)]$	2.82	14.55	3.925	0.001

8 **Table 3 : Discretization of variances of measured parameters.**

9

10 *Variance of the fluctuation between the values measured and the deterministic trend*
11 $Var[Z_i(x) - t_{Z_i}(x)]$ *:*

12 By comparing the fluctuation variance values $Var[Z_i(x) - t_{Z_i}(x)]$ with those of table 2
13 (without taking spatial variability into account), we observe a reduction of variance only for
14 parameter r, the only parameter for which a deterministic trend of evolution as a function of
15 depth was identified.

16 *Variance of the measurement error* $Var[e_{Z_i}]$ *:*

17 For parameters r and R, we evaluated the measurement error $Var[e_{Z_i}]$ for each of the 62
18 Schmidt hammer tests using equation [8] and we adopted the mean of these 62 values as
19 representative of the measurement error $Var[e_{Z_i}]$ for r and R.

20 For parameter φ_b, the low measurement error is due to the good alignment obtained
21 during the shear tests on a smooth joint, and the experimental shear strength values as a
22 function of normal stress.

23 We omitted the measurement error for $Z2$ given the precision of the profilometer, which
24 appeared valid given the low variance of the fluctuation $Var[Z_i(x) - t_{Z_i}(x)]$.

25 *Variance of the fluctuation* $Var[w_{Z_i}(x)]$ *:*

26 Regarding the variance of the fluctuation $Var[Z_i(x) - t_{Z_i}(x)]$, the share of the
27 measurement error $Var[e_{Z_i}]$ remained low in comparison to the share of the residue
28 corresponding to $Var[w_{Z_i}(x)]$.

4.2.2 Modeling of the input parameters of the Barton and Choubey model at the scale of the joints intersected by a borehole

31 The input parameters of the Barton and Choubey model at the scale of the joints
32 intersected by a borehole were evaluated from measured parameters, using the empirical
33 models of equations [2], [3] and [4].

1   Table 4 presents a synthesis of the statistical analysis of the input parameters of Barton
2   and Choubey's model (without taking spatial variability into account):

3

Parameter	JRC [-]	JCS [MPa]	φ_r [°]
Mean	8.1	95	27.1
Standard deviation	2.7	38	3.3
Variation coefficient	0.33	0.40	0.12
Variance	7.1	1444	10.6

4   **Table 4 : Statistical data of the input parameters of Barton and Choubey's model (without**
5   **accounting for spatial variability).**

6

7   Table 5 presents the results of applying the analytical formulas obtained by Taylor series
8   linearization to estimate expected value (equations [11] to [13]) and variance (equations [14 to
9   19]) of the input parameters of Barton and Choubeys' criterion at the scale of the joints:

10

Parameter, $Z_{di}(x)$	$JRC(x)$	$JCS(x)$	$\varphi_r(x)$
Expected value, $E[Z_{di}(x)]$	8.1	129	29.2
Variance, $Var[Z_{di}(x)]$	7.1	326	4.2

11   **Table 5 : Expected value (mean) and Variance of the input parameters of Barton and Choubey's**
12   **model at the scale of the joints.**

13

14   The comparison of the variances of Table 4 with those of Table 5 permits highlighting
15   the effects of reducing variance associated with a deterministic trend observed on the
16   measured parameters.

17   This reduction of variance is zero for parameter $JRC(x)$, itself defined as a function of
18   parameter $Z_2(x)$ which presents a trend that does not change as a function of depth in the
19   borehole.

20   Parameters $\varphi_r(x)$ and $JCS(x)$ present reduced variance as they are defined as a function
21   of the rebound value of the altered joints $r(x)$ which present an in increasing trend as a
22   function of depth. This explains the evolution of the mean (or expected value) of parameters
23   $JCS(x)$ and $\varphi_r(x)$.

4.2.3 Modeling the input parameters of the Barton and Choubey's model at the scale concerned by the limit state

26   We consider a borehole length $L = 10$ m as representative of the scale concerned by the
27   limit state (scale of the structure) for the input parameters of the Barton and Choubey's
28   model.

29   The expected values $E[…]$ of the input parameters of the Barton and Choubey's criterion
30   at the scale of the structure are obtained directly from equations [21] to [23] defined as a
31   function of the deterministic trend of the parameters measured. These values are presented in
32   Table 7.

14

1   To evaluate the variance Var[…] of the input values of the Barton and Choubey model at
2   the scale of the structure, it is necessary beforehand to build the variograms of the parameters
3   measured to then obtain the variance reduction coefficient of the parameters at the scale of the
4   structure (equations [24 to 28]).

5   Here, the case study is a gravity dam. For this type of dam, there is rarely more than one
6   borehole along the same analyzed profile. Moreover, the distance between boreholes is
7   generally of the same order of magnitude as the size of the area of the limit state considered
8   (or even larger). All these conditions limit the interest of a variogram analysis in a horizontal
9   direction. Thus, variograms were constructed along the vertical direction (corrected for
10   inclined boreholes) which is also more practical as regards to the data available along a
11   borehole.

12   Figure 2 and Table 6 show the variograms obtained for the measured parameters:
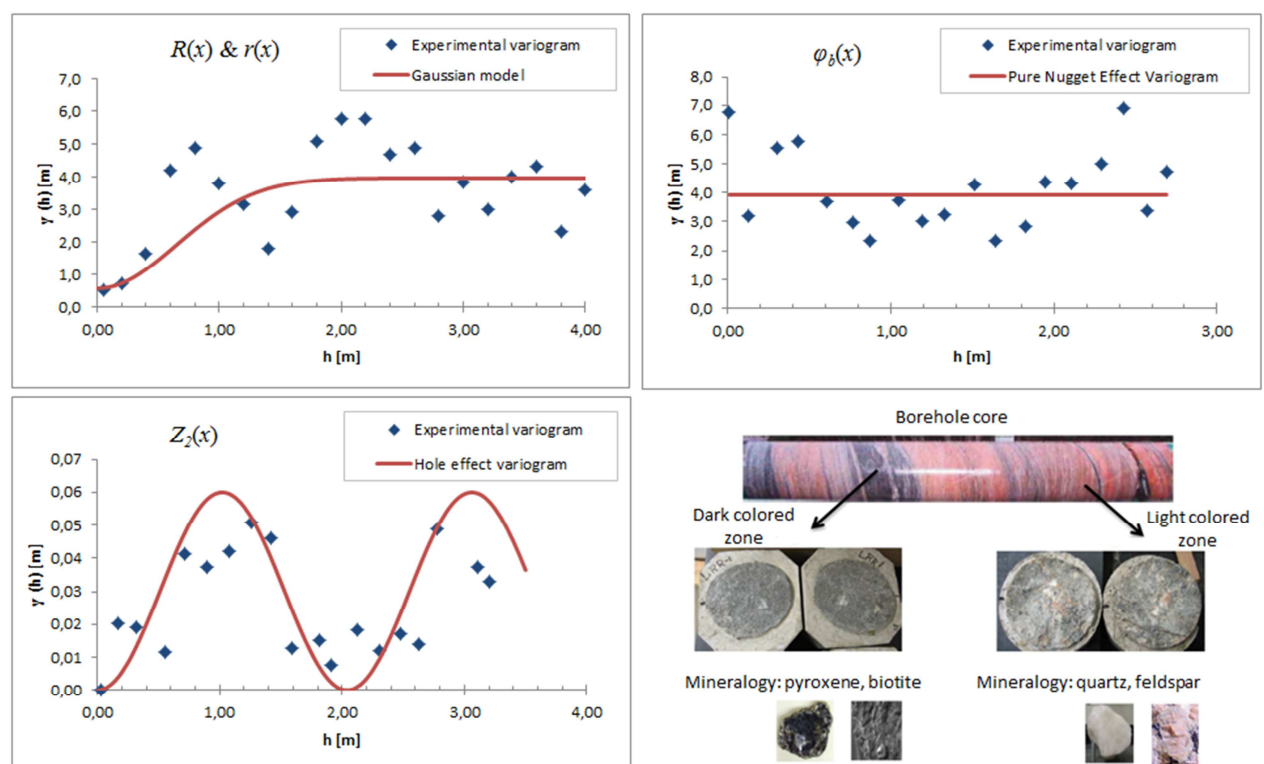
13

Figure 2: Variograms obtained for the parameters measured.

14

15

16

17

1

Parameter	Variogram model		Variograms parameters
$R(x)$ & $r(x)$	Gaussian	$\gamma(h) = c \cdot \left(1 - e^{-\left(\frac{h}{a}\right)^2}\right) + c_0$	c = 3.4 c_0 = 0.59 a = 0.92
$\varphi_b(x)$	Nugget	$\gamma(h) = c_0$	c_0 = 3.93
$Z_2(x)$	Hole effect	$\gamma(h) = c + (c_0 - c) \cos\left(h\frac{\pi}{a}\right)$	c = 0.03 c_0 = 0 a = 1.02

2   **Table 6 : Variogram models of the measured parameters**

3

4   Given the low number of $r(x)$ values, we aggregated them with the values of $R(x)$. This
5   was justified knowing that it is the same type of measurement and that the variograms are
6   built for the fluctuation between the measured values and the deterministic trend.

7   Part of the wave effect of the experimental variogram could be interpreted by the
8   influence of the alternation of light-colored zones (richer in quartz-feldspar) and dark ones
9   (richer in mafic minerals). This wave effect is increased for the roughness parameter Z_2,
10   which may be due to the superficial nature of the laser profilometer measurements (the nature
11   of the rebound measurements is less superficial given the propagation of impact energy in the
12   sample).

13   It is noteworthy that when the mean of a variable varies as a function of depth, the field is
14   no longer stationary. The variance reduction coefficient is therefore estimated for the
15   fluctuation variable (which can be considered as stationary) between the values measured and
16   the deterministic trend.

17   The variance reduction coefficients evaluated from the variograms are: $\Gamma_r^2(10\text{ m}) =$
18   $\Gamma_R^2(10\text{ m}) = 0.15$; $\Gamma_{Z_2}^2(10\text{ m}) = 0.43$; $\Gamma_{\varphi_b}^2(10\text{ m}) = 1$.

19   Table 7 presents the results of applying the analytical formulas obtained by Taylor series
20   linearization (and from the variograms) to estimate the expected value (equations [21 to 23])
21   and the variance (equations [23 to 27]) of the input parameters of the Barton and Choubey's
22   criterion at the scale of the structure:

23

Parameter, $Z_{Li}(L)$	$JRC_L(L)$ [-]	$JCS_L(L)$ [MPa]	$\varphi_{rL}(L)$ [°]
Expected value, $E[Z_{Li}(L)]$	8.1	129	29.2
Variance, $Var[Z_{di}(L)]$	2.9	107	4.2

24   **Table 7 : Expected value (mean) and Variance of the input parameters of the Barton and Choubey's**
25   **model at the scale of the structure.**

26

1   Figure 3 summarizes the results obtained for the variance reduction analysis expressed as
2   the standard deviation in order to keep the same unit to compare the parameters:

3   -   the first term of each graph corresponds to the dispersion of the values without taking
4   spatial variability into account;
5   -   the second term corresponds to the dispersion of the fluctuation of values around the
6   deterministic trend as a function of depth (x);
7   -   the third term is obtained by assigning the second term by the variance reduction
8   coefficient evaluated for depth (L).
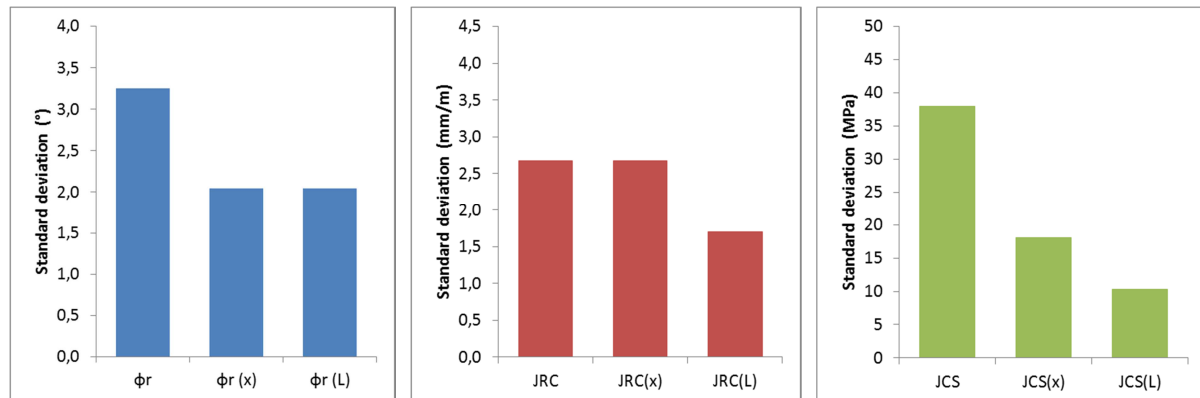
9

Figure 3: Reduction of the standard deviation of the Barton and Choubey parameters.

13   We provide the following explanations for these reductions of variance:

14   -   for $\varphi_r(x)$ and $JCS(x)$, the reduction of variance stems from the definition of a trend as
15   a function of depth for parameter $r(x)$;
16   -   for $JRC(L)$ and $JCS(L)$, the reduction of variance stems from the spatial correlation
17   evaluated from the variograms.

18 4.3   Results of application to the stability analysis

19   In this application, *Phase²©* geomodeler was used to build the geological model in 2D.
20   Using a 2D model can be satisfactory in the case where the stability of gravity dam
21   foundations is analyzed in 2D.

22   We focus on the limit state of shear strength on the joints of the rock mass. The condition
23   of joint shear strength consists in verifying that the shear strength remains higher than the
24   tangential stresses along the joints.

25   The *Phase²©* geomodeler is based on the finite elements method and uses the Shear
26   Strength Reduction (SSR) method to analyze this limit state of joint shear strength, and more
27   generally, for analyzing the stability of rock masses (Griffits and Lane 1999).

28   For the reliability analysis, we use the probabilistic module integrated in the *Phase²©*
29   geomodeler. It is defined in random variables and estimates the probability of failure using the
30   Point-Estimate Method (Rosenblueth, 1975). This permits showing the impact that taking
31   variance reduction into account can have on estimating the probability of failure.

1   The probabilistic module of the *Phase^2©* software is limited to the Mohr-Coulomb
2   model. The Barton and Choubey's model was then linearized in the range of normal stresses
3   developed in the rock mass in order to implement Mohr-Coulomb's linear model.

4   In the application, we considered the shear strength parameters as random variables. Two
5   sets of random variables were considered according to two configurations: with and without
6   taking variance reduction into account. In order to facilitate the comparison between these
7   two configurations, we considered only static actions taken as deterministic, including weight,
8   the hydrostatic pressure and uplift (the latter without taking a drainage system into account).

9   Table 8 presents the probability laws considered to represent the random variables
10   WITHOUT taking variance reduction into account.

11

Random variables WITHOUT taking variance reduction into account	JRC [-]	JCS [MPa]	φ_r [°]
Type of probability law	Lognormal	Weibull	Weibull
Mean	8.1	104	28
Standard deviation	2.7	29	2.9

12   **Table 8 : Random variables WITHOUT taking variance reduction into account.**

13

14   To determine the type of probability law of the random variables used in the stability
15   analysis, we used Monte-Carlo simulations: a probability distribution was fitted to the
16   statistical data of the parameters measured (R, r, φ_b and Z_2) to then generate a sample
17   comprising a high number of values for the input parameters of the Barton and Choubey
18   model so as to finally fit a probability law to these parameters.

19   For the scale associated with the limit state, we considered a depth (L) of 3.5 m given the
20   width of the dam at its base and the dip of the joint set developed along the foliations. Table 9
21   presents the laws of probability considered to represent the random variables WITH the
22   variance reduction taken into account (at the scale of the structure).

23

Random variables WITH the variance reduction taken into account	JRC_L (3,5 m) [-]	JCS_L (3,5 m) [MPa]	φ_{rL} (3,5 m) [°]
Type of probability law	Lognormal	Weibull	Weibull
Mean	8.1	85.7	26.9
Standard deviation	1.8	6.5	1.99

24   **Table 9 : Random variables WITH the variance reduction taken into account**

25

26   It is noteworthy that the values of Table 8 and Table 9 differ from those of Table 5 and
27   Table 7, respectively. These differences essentially stem from the depth (L) used to represent
28   the scale associated with the limit state or scale of the structure ($L = 10$ m to illustrate the
29   method proposed and $L = 3.5$ m for the specific application to the stability analysis);

30   Figure 4 shows the result of a simulation of joints in a rock mass and the displacements
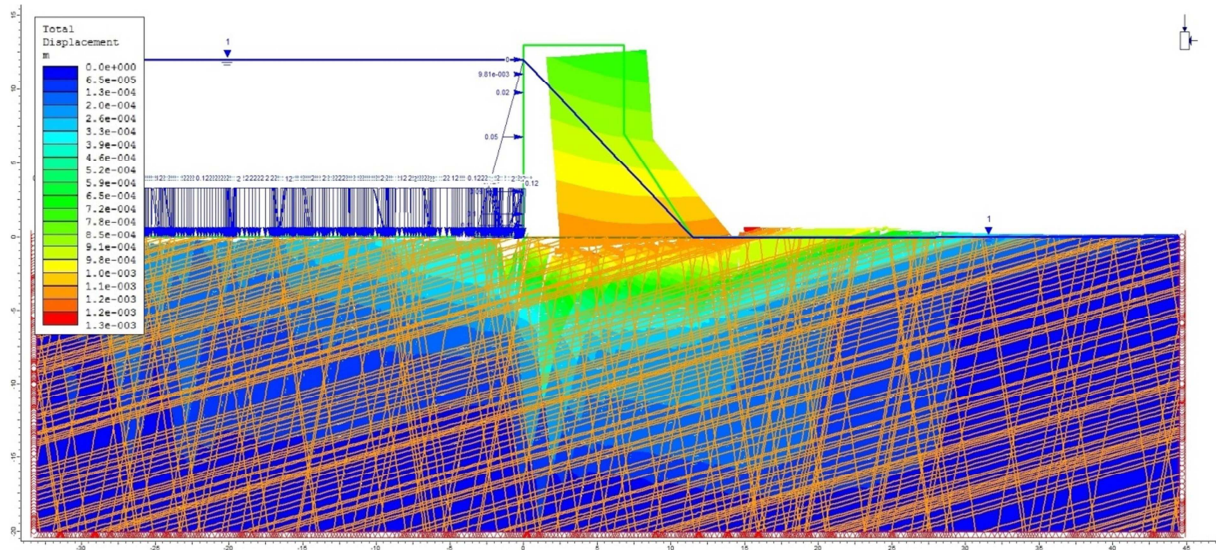31   obtained.

1

2

3 **Figure 4 : Results of a simulation of rock mass joints and the associated displacement field.**

4

5   The probability of failure evaluated for the case of random variables WITHOUT taking
6 into account variance reduction is 2×10^{-6}. For this study, taking variance reduction into
7 account led to reducing the probability of failure by several orders of magnitude ($<10^{-8}$). Thus
8 this application permits highlighting the impact that taking variance reduction (and the
9 associated variance reduction) into account can have on the probability of failure evaluated in
10 a reliability analysis.

11 # 5   DISCUSSION ON THE METHODOLOGY AND ON THE RESULTS

12 ## 5.1   Discussion on the methodology

13   The methodology proposed permits analyzing the spatial variability of shear strength
14 along the joints of rock masses. In particular it allows taking into account the effects of
15 variance reduction by identifying a deterministic trend varying in depth and by analyzing
16 spatial correlation on the basis of geostatistical analysis. Taking into account of the variance
17 reduction of the shear parameters involved at the limit-state scale (scale of the structure) can
18 lead to reduce the probability failure commonly assessed by a reliability analysis.

19   The methodology proposed is based on the Barton and Choubey's criterion that brings
20 into play a greater amount of data than an approach based only on direct shear tests. Indeed,
21 the methodology proposed is founded on an experimental approach leading to the generation
22 of large sets of shear strength properties, using a simple and inexpensive experimental
23 protocol (employing a laser profilometer, a portable shear test apparatus and a concrete
24 sclerometer). The statistical sample of shear strength properties thus generated can then be
25 subjected to an analysis and spatial variability modeling.

26   The proposed methodology uses an approximation by Taylor series linearization for
27 estimating the expected value and the variance of the input parameters of the Barton and
28 Choubey criterion. The accuracy of this approximation is conditioned by the linearity of the
29 concerned formulas. However, this approximation has the advantage to allow an analytical

1   calculation of the expected value and the variance of the variables analyzed, which is more
2   practical in engineering.

3   The evaluation of shear strength requires the evaluation of a larger number of measured
4   parameters and the use of empirical models to evaluate the parameters of the Barton and
5   Choubey's criterion. Thus the study focused on identifying and characterizing the weight of
6   the measured parameters on the evaluated parameters (parameters of the Barton and
7   Choubey's criterion). For each parameter, the methodology suggested sought to separate the
8   uncertainties that could be explained by spatial localization (with a deterministic trend) from
9   the uncertainties linked to the measurements and from those linked to the models used.

10   The study also allowed taking into account an effect of scale by integrating measurement
11   variability (done at the scale of the joints intersected by the borehole) in a larger volume
12   associated with the limit state concerned (or the scale of structure). However, the effect of
13   physical scale associated with the size of the samples was not considered in this methodology
14   and therefore provides a future path for this work. In particular, it will require the utilization
15   of experimental resources making it possible to carry out tests on much larger rock surfaces
16   than those tested in the boreholes.

17 ## 5.2   Discussion on the results

18   The case study analyzed demonstrated the applicability of the method proposed using real
19   experimental data and for a rock mass foundation of a real dam.

20   The number of test data available in the case study is relatively large, but it might not be
21   sufficient for an accurate statistical or geostatistical analysis. Despite the statistical
22   uncertainty which may be generated by the number of experimental data available, the
23   application of the proposed method can yield a reduction of the variance of the variable
24   analyzed by taking into account the spatial variability.

25   Regarding the case study, it was possible to quantify the measurement error for the
26   rebound tests. The laser profilometer provided a very high level of precision for the roughness
27   measurements, which led to considering the raw measurement error as negligible.
28   Nonetheless, the impact of the protocol used to obtain the roughness measurements could be
29   analyzed by considering several possible profiles of the same sample.

30   The model error was not quantified in the case study. It is possible that the model error is
31   more significant for the estimation of φ_r and of JCS, with empirical models determined as a
32   function of φ_b, R and r for φ_r and as a function of R only for JCS. The model error for JRC is
33   probably less significant (Z_2 measured quantitatively on roughness profiles given by the
34   Barton and Choubey, 1977). Nevertheless, the methodology proposed permitted incorporating
35   these errors in every case when they were quantified.

36   Taking spatial evolution into account (in this case as a function of depth) via a
37   deterministic trend led to a significant reduction of the variance of the variable analyzed.
38   Regarding the case study, this trend was described only for the rebound value of the altered
39   joints $r(\mathrm{x})$, leading to a significant reduction of the variance associated with variables φ_r and
40   JCS. Taking into account the spatial correlation allowed obtaining an additional reduction of
41   variance (more significant in the case when the contribution of the deterministic trend was
42   slight).

43   The stability analysis performed for the rock mass corresponded to an initial estimation
44   and served to provide an illustrative value. Indeed, several simplifying hypotheses were

1 employed, such as 2D modeling of the massif which led to omitting the kinematics of blocks
2 in 3D, and modeling uplifts without taking into account a drainage system.

3   Therefore the stability calculation results cannot be retained as absolute values, since
4 only the relative values between the results with and without taking variability into account
5 should be considered. In spite of the hypotheses adopted, this stability analysis was a direct
6 application of the results of the methodology proposed and permitted highlighting the
7 considerable impact that taking variance reduction into account can have on estimating the
8 probability of failure.

9 ## 6   CONCLUSIONS

10   We developed an approach that analyzes the spatial variability of the shear strength of
11 joints using the input parameters of the Barton and Choubey's model. This approach was
12 based on using the georeferenced data of these parameters characterizing the same set of
13 joints along a borehole. It allowed identifying spatial organization and evaluating the variance
14 reduction of the parameters involved at large scale by identifying a deterministic trend
15 varying in depth and a spatial correlation deduced from a variographic analysis.

16   To evaluate the pertinence and applicability of this approach, we applied it in the case
17 study of a rock mass making up the rock mass of a gravity dam. In this application, we
18 focused on a set of joints intersected by a vertical, oriented borehole.

19   Taking variance reduction into account in the case study led to significantly reducing the
20 probability of failure. Given the simplified nature of the reliability analysis performed in this
21 study, we consider performing a fuller reliability analysis using a numerical 3D model, taking
22 into account the random character of hydraulic stresses, the direct use of the Barton and
23 Choubey's criterion and the explicit inclusion of random fields.

24

25 ## ACKNOWLEDGEMENTS

29

1   APPENDIX A: TEST DATA

2   Test data used in this article is summarized in Table A.1.

3

Borehole	Depth [m]	R [-]
FVG2	3,00	49,80
FVG2	4,50	48,60
FVG2	4,25	47,95
FVG2	4,25	46,97
FVG2	4,25	48,30
FVG2	7,58	44,34
FVG2	7,25	45,77
FVG2	8,25	44,97
FVG2	8,25	44,37
FVG2	8,25	48,10
FVG2	8,75	45,37
FVG3	0,50	43,17
FVG3	0,80	45,77
FVG3	1,12	49,40
FVG3	2,12	48,70
FVG3	1,87	51,00
FVG3	3,18	47,07
FVG3	3,91	46,15
FVG3	3,87	47,70
FVG3	3,87	47,00
FVG3	4,52	49,30
FVG3	4,87	47,70
FVG3	5,37	48,20
FVG3	5,44	49,80
FVG3	4,87	49,80
FVG3	5,54	50,20
FVG3	5,59	49,40
FVG3	4,87	49,40
FVG3	5,69	50,50
FVG3	4,87	50,00
FVG3	5,87	50,40
FVG3	6,72	50,10
FVG3	6,77	50,20
FVG3	5,87	50,80
FVG3	6,87	49,90
FVG3	6,87	50,40
FVG3	6,97	49,20
FVG3	6,87	49,80

Borehole	Depth [m]	r [-]
FVD1	2,20	41,94
FVD1	3,70	39,48
FVD1	3,70	43,89
FVD1	6,99	51,60
FVD1	6,99	48,50
FVD2	0,39	37,39
FVD2	0,39	35,97
FVD2	4,21	44,97

Borehole	Depth [m]	φ_b [°]
FVG2	2,00	33
FVG2	2,03	35
FVG2	2,85	32
FVG2	3,65	32
FVG2	4,45	29
FVG2	4,55	34
FVG2	4,70	35
FVG2	4,90	34
FVG2	7,65	33
FVG2	7,81	32
FVG2	8,70	33
FVG3	2,10	35
FVG3	2,38	34
FVG3	3,18	31
FVG3	3,91	33
FVG3	4,32	28
FVG3	4,47	33
FVG3	4,67	30
FVG3	4,85	31

Borehole	Depth [m]	Z_2 [-]
FVG3	0,50	0,168
FVG3	0,80	0,180
FVG3	1,12	0,156
FVG3	1,41	0,156
FVG3	1,65	0,225
FVG3	2,38	0,168
FVG3	2,48	0,145
FVG3	1,87	0,135
FVG3	2,93	0,156
FVG3	2,87	0,156
FVG3	3,18	0,156
FVG3	3,27	0,214
FVG3	3,27	0,207
FVG3	3,91	0,240
FVG3	3,87	0,168
FVG3	4,87	0,224
FVG3	6,43	0,193
FVG3	5,87	0,180
FVG3	7,61	0,268

FVD1	0,80	57,20
FVD1	2,20	57,20
FVD1	2,50	56,00
FVD1	2,86	56,00
FVD1	2,86	56,20
FVD1	3,70	56,10
FVD1	3,70	55,40
FVD1	6,00	57,10
FVD1	6,50	57,10
FVD1	6,50	56,50
FVD1	6,99	55,80
FVD1	6,99	54,75
FVD1	7,30	53,77

Table A. 1 : Test data used in this article

REFERENCES

AFTES (2003). « Recommandations relatives à la caractérisation des massifs rocheux utile à l'étude et à la réalisation des ouvrages souterrains ». Tunnels et Ouvrages souterrains N° 177: 30p.

ASTM D5607-08 (2008). Standard Test Method for Performing Laboratory Direct Shear Strength Tests of Rock Specimens Under Constant Normal Force. ASTM International, West Conshohocken, PA, 2008.

Matheron G. (1970) La théorie des variables régionalisées et ses applications Cahiers du Centre de Morphologie Mathématiques de Fontainebleau Fascicule n° 5, 212 pages.

Barton N.R. & Choubey V. (1977). « The shear strength of rock joints in theory and practice », *Rock Mech Rock Eng.*, vol. 10, n° 1-2, 1977, p. 1-54.

Blès, J.-L. et Feuga B. (1981). *La fracturation des roches*. BRGM, Manuel et méthodes n°1, vol.1, 160p. 1981.

Carvajal C., Peyras L., Bacconnet C., Bécue J-P (2009). « Probability Modelling of Shear Strength Parameters of RCC Gravity Dams for Reliability Analysis of Structural Safety". *European Journal of Environmental and Civil Engineering*, 2009 vol.13 No.1, pp.91-119.

CFBR (2012). *Recommandations pour la justification de la stabilité des barrages-poids*. Comité Français des Barrages et Réservoirs, 2012.

Deere, D. U. and R. P. Miller (1966). Engineering classification and index properties for intact rock. Report AFWL-TR-65-116. Air Force Weapons Laboratory (WLDC). Kirtland Air Force Base. New Mexico 87117.

Duzgun, H.S.B., Yucemenb, M.S., Karpuzc, C. (2002). "A probabilistic model for the assessment of uncertainties in the shear strength of rock discontinuities". *International Journal of Rock Mechanics & Mining Sciences*, vol.39, 2002, p. 743–754.

23

1   Favre J.L. (2004). *Sécurité des ouvrages / Risques : Modélisation de l'incertain, fiabilité,*
2   *analyse des risques*, Paris, Ellipses, 2004.

3   Gyenge, M. and G. Herget (1977). Determination of strength properties of rock
4   discontinuties by direct Shear test. Laboratory tests for design parameters. Canada,
5   Canmet Report. 77-26.

6   Grasselli, G. and P. Egger (2003). "Constitutive law for the shear strength of rock joints
7   based on three-dimensional surface parameters". International Journal of Rock
8   Mechanics and Mining Sciences 40(1): 25-40.

9   Gravanis, E., Pantelidis, L., Griffiths, D.V. (2014). "An analytical solution in
10   probabilistic rock slope stability assessment based on random fields". International
11   Journal of Rock Mechanics & Mining Sciences, vol.71, 2014, p. 19–24.

12 Griffiths, D.V. and Lane, P.A. (1999). "Slope stability analysis by finite elements".
13   Geotechnique, vol. 49, no. 3, pp.387-403.

14 Hoek & Brown (1980). Underground excavation in rock. London, Instn Min. Metall.

15 ISRM (1978). "Suggested methods for the quantitative description of discontinuities in
16   rock masses". Int. J. Mech. Min. Sci & Geomech. Abstr Vol 15: pp 319-368.

17 Jaboyedoff, M., F. Philippossian, et al. (1996). "Distribution spatiale des discontinuités
18   dans une falaise, approche statistique et probabilistique". Short Course-
19   QUANTERRA: International independant center of climate change impact and
20   natural risk analysis in mountainous area: 13 p.

21 Merrien-Soukatchoff, V. and T. Korini (2011). "Use of an integrated discrete fracture
22   network code for stochastic stability analyses of fractured rock masses" Rock
23   Mechanics and Rock Engineering, 2012, Volume 45, Issue 2, pp 159-181.

24 Panet, M. (1976). *La Mécanique des roches appliquée aux ouvrages de génie civil*. Paris :
25   Presses de l'Ecole Nationale des Ponts et Chaussées, 1976, 235p.

26 Peyras L., Merckle S., Royet P., Bacconnet C., Ducroux A. (2010). Study on a semi-
27   probabilistic method for embankment hydraulic works – Application to sliding
28   mechanism. European Journal of Environmental and Civil Engineering, Vol. 14, n°5.
29   pp.669-691

30 Phoon, K. K. and F. H. Kulhawy. (1999). "Characterization of geotechnical variability".
31   *Canadian Geotechnical Journal,* vol.36, n°4, p.612-624, 1999.

32 Rosenblueth, E. (1975) Point estimates for probability moments, in Proceedings of the
33   National Academy of Sciences, Vol. 72 (10), pp. 3812–3814.

34 Shamekhi, E., Tannant, D.D. (2015). "Probabilistic assessment of rock slope stability
35   using response surfaces determined from finite element models of geometric
36   realizations". Computers and Geotechnics, vol.69, 2015, p. 70–81.

37 Sow, D. (2015). Variabilité spatiale de la résistance au cisaillement des discontinuités des
38   fondations rocheuses de barrages. Université Blaise Pascal - Clermont-Ferrand II,
39   2015. PhD thesis, French.

40 Sow D, Rivard P, Peyras L, Breul P, Moradian Z.A., Bacconnet C, Ballivy G. (2015).
41   Comparison of Joint Shearing Resistance Obtained with the Barton and Choubey
42   Criterion and with Direct Shear Tests. Technical Note, Rock Mechanics and Rock
43   Engineering, pp 1-5.

1   Tse R., Cruden D.M. (1979). "Estimating joint roughness coefficients". International
2   Journal of Rock Mechanics and Mining Sciences & Geomechanics Abstracts.
3   Vol.16, n°5 (1979), pp. 303-307.

4   Vanmarcke, E. H. (1983). *Random fields: Analysis and Synthesis* (Revised and Expanded
5   New Edition 2010). London: MIT Press, 372p., 1983. ISBN: 0262220261.

6   Wang Y, Cao Z. (2013). "Probabilistic characterization of Young's modulud of soil using
7   equivalent samples". Engineering Geology 159 (2013), pp. 106-118.

8   Wang Y., Aladejare A.E. (2015). "Selection of site-specific regression model for
9   characterization of uniaxial compressive strength of rock". International Journal of
10   Rock Mechanics & Mining Sciences 75 (2015), pp. 73–81.

11 Wang Y, Cao Z., Li D. (2016). "Bayesian perspective on geotechnical variability and site
12   characterization". Engineering Geology 203 (2016), pp. 117–125.

13

14